Applied Physics Letters

Enhancement of spin–orbit torque in Pt/Co/HfOx heterostructures with voltage-controlled oxygen ion migration

Cite as: Appl. Phys. Lett. **122**, 122403 (2023); https://doi.org/10.1063/5.0139443
Submitted: 20 December 2022 • Accepted: 06 March 2023 • Published Online: 20 March 2023

S. Wu, T. L. Jin, F. N. Tan, et al.

AIP Publishing

Applied Physics Letters ARTICLE scitation.org/journal/apl

Enhancement of spin–orbit torque in Pt/Co/HfOx heterostructures with voltage-controlled oxygen ion migration

Cite as: Appl. Phys. Lett. **122**, 122403 (2023); doi: 10.1063/5.0139443
Submitted: 20 December 2022 · Accepted: 6 March 2023 ·
Published Online: 20 March 2023

View Online Export Citation CrossMark

S. Wu, T. L. Jin, F. N. Tan, C. C. I. Ang, H. Y. Poh, G. J. Lim, and W. S. Lew[a)]

AFFILIATIONS

School of Physical and Mathematical Sciences, Nanyang Technological University, 21 Nanyang Link, Singapore 637371

Note: This paper is part of the APL Special Collection on Magneto-ionic and electrostatic gating of magnetism: Phenomena and devices.

[a)]**Author to whom correspondence should be addressed:** wensiang@ntu.edu.sg

ABSTRACT

Spin–orbit torque (SOT) induced magnetization switching and SOT modulation by interfacial coupling exhibit good potential in spintronic devices. In this work, we report the enhancement of damping-like field and SOT efficiency of up to 60% and 23%, respectively, in perpendicularly magnetized Pt/Co/HfO_x heterostructures over a Pt/Co system at an optimal thickness of 2 nm HfO_x. The SOT improvement is primarily attributed to the interfacial oxidization of the Co layer, and the strength is tunable via voltage-induced oxygen ion migration at the Co/HfO_x interface. Our measurement reveals that by controlling gate voltages, the Co oxidation can be increased, which leads to the SOT efficiency enhancement. Our work promotes the SOT enhancement and modulation by oxidation effects for energy-efficient spintronic devices.

Spin–orbit torque (SOT) has been intensely pursued and developed in recent years for efficient magnetization switching. Specifically, spin–orbit torque magnetic random-access memory (SOT-MRAM) shows good performance with fast access time, low energy consumption, and good endurance.[1,2] SOT is mainly induced by spin–orbit coupling (SOC) through the spin Hall effect (SHE)[3–6] or the interfacial Rashba effect in heavy metal (HM)/ferromagnet (FM) heterostructures,[7] injecting spin-polarized electrons from the HM into the adjacent FM layer. The local magnetic moment in the FM experiences spin torque via the angular momentum exchange and undergoes magnetization switching at low energy cost.[8,9] Such a structure allows separate paths for reading and writing currents, thereby improving the performance and endurance of the memory device.[10] Various approaches have been proposed for SOT efficiency enhancement. Thus far, enhanced SOT efficiency has been achieved by implementing rare-earth metals,[11,12] optimizing layer thicknesses,[13] and modulating the HM/FM interface.[14–16] Research has shown that the magnetic anisotropy of FM layers can be modified via inducing surface charges[17,18] or orbital occupancy[19–21] by interfacing with an oxide layer. Aside from utilizing SOT to reduce energy consumption, voltage-controlled oxygen migration is another technique to reduce the energy barrier for magnetization switching. The electric-field-driven interfacial oxygen mobility can affect both the SOT strength and sign. The prospect of the combination of SOT and oxygen migration has incited attempts to use ionic liquid or under elevated temperatures.[22–28] However, more research on the oxidation effects at the interfaces of the voltage-controlled magnetism in FM/oxide systems needs to be investigated.

In this work, we report the enhancement of the damping-like field and SOT efficiency of up to 60% and 23%, respectively, in a Pt/Co system using the HfO_x capping layer to form Co oxidation, which includes a study on the thickness of the HfO_x layer. We further verify this enhanced SOT by applying voltages across the Pt/Co/HfO_x structure, which allows the O^{2-} migration from HfO_x to the Co layer. By using voltage-controlled oxygen ion modulation of interfacial oxidation, we show that the gate voltage affects not only coercivity and anisotropy fields but also the SOT efficiency at room temperature, which is comparable with those reported ionic control limited effects.[29] Moreover, we show the gating effect under specific gate voltages with a solid HfO_x layer rather than using the liquid,[30] which is more compatible with an energy-efficient MRAM architecture.

A stack structure comprising Pt (5 nm)/Co (1.4 nm)/HfO_x (t_{HfO}) was prepared, as well as a control sample, Pt (5 nm)/Co (1.4 nm)/Ti (2 nm) without an HfO_x ($t_{HfO} = 0$ nm) layer. Note that the 2 nm Ti capping layer in the control sample stack is intended to protect the Co layer from oxidation. Both stacks were grown over a 2 nm Ti seed layer for better adhesion on a thermally oxidized Si substrate. All the layers were deposited by using magnetron sputtering at room temperature in an ultra-high vacuum chamber with a base pressure of 5×10^{-8} Torr. The schematic of the thin film stack is shown in Fig. 1(a). The hysteresis behavior of the films was measured by using a vibrating sample magnetometer (VSM). Hall cross devices of $10 \times 100\ \mu m^2$ were fabricated using electron-beam lithography and argon ion milling techniques. Contact pads comprising Ti (10 nm)/Cu (50 nm)/Ti (10 nm) were fabricated using a liftoff process. The magnetic properties of the devices were electrically characterized by anomalous Hall effect (AHE) measurements. The SOT efficiency was determined by harmonic Hall voltage measurement by using a Keithley 6221 AC source and a 7265 dual-phase DSP lock-in amplifier.[31]

Figure 1(b) shows the magnetic hysteresis (M–H_z) loops of the thin films with the HfO_x thicknesses varying from 0 to 3.5 nm by sweeping the magnetic field (H_z) along the out-of-plane direction. The hysteresis loops indicate the presence of perpendicular magnetic anisotropy (PMA). However, the hysteresis loops of the HfO_x samples have a reduced coercivity compared to the control sample as shown in Fig. 1(c). The saturation magnetization (M_s) shows a sharp decrease from 926 ± 12 ($t_{HfO} = 0$ nm) to 634 ± 6 emu/cm^3 ($t_{HfO} = 2$ nm) and remains basically the same after 2 nm thickness of HfO_x as shown in Fig. 1(d). Therefore, the subsequent investigation was performed on devices with a 2 nm HfO_x capping layer. Since M_s is mainly determined by the total magnetic moment of the Co layer, it is reasonable to attribute the lower H_c and M_s in the HfO_x sample to some intrinsic factors such as interfacial roughness, hybridization at the heavy metal/ferromagnetic metal interface, and oxidation of the ferromagnetic layer. Moreover, the reduction of H_c and M_s in the HfO_x sample is also due to the Co oxidation,[32] which is formed via oxygen diffusion into the Co layer at the Co/HfO_x interface.

To support the occurrence of Co oxidation at the Co/HfO_x interface, the magnetic dead layer measurements were performed. Figure 2(a) demonstrates the downward migration of oxygen to form CoO_x. By quantifying the M_s of the films at different Co thicknesses using the VSM, the magnetic dead layer thicknesses were obtained from the linear extrapolation of the M_s to zero, as shown in Fig. 2(b). The lower M_s of the HfO_x sample compared to the control sample with identical Co thickness indicates more oxidized Co atoms. The Co interfacing with HfO_x has a ~0.45 nm dead layer, while the Co interfacing with Ti has a ~0.2 nm dead layer. Hence, the results show that a layer of CoO_x is formed when HfO_x is deposited onto the Co interface, which will lead to an enhancement of the Rashba effect. In addition, CoO_x is known to be an insulating antiferromagnetic material, which may affect the SOT efficiency.[33]

Figure 3(a) shows an optical micrograph of the Hall cross device of a $10 \times 100\ \mu m^2$ structure. Figure 3(b) shows the anomalous Hall resistance R_{AHE}–H_z loops of the measured Hall cross devices. The change of the R_{AHE} (ΔR_{AHE}) is lower in the HfO_x sample compared to the control sample. Subsequently, the first and second harmonic Hall voltage measurements were carried out by sweeping an external in-plane magnetic field in two directions: along and transverse to the current directions.[31,34] The measured harmonic Hall voltages for the Pt/Co/HfO_x sample are shown in Fig. 3(c). M_{up} and M_{down} represent the magnetization directions of the PMA device. Based on the measured Hall voltage results, the damping-like field is obtained as[31]

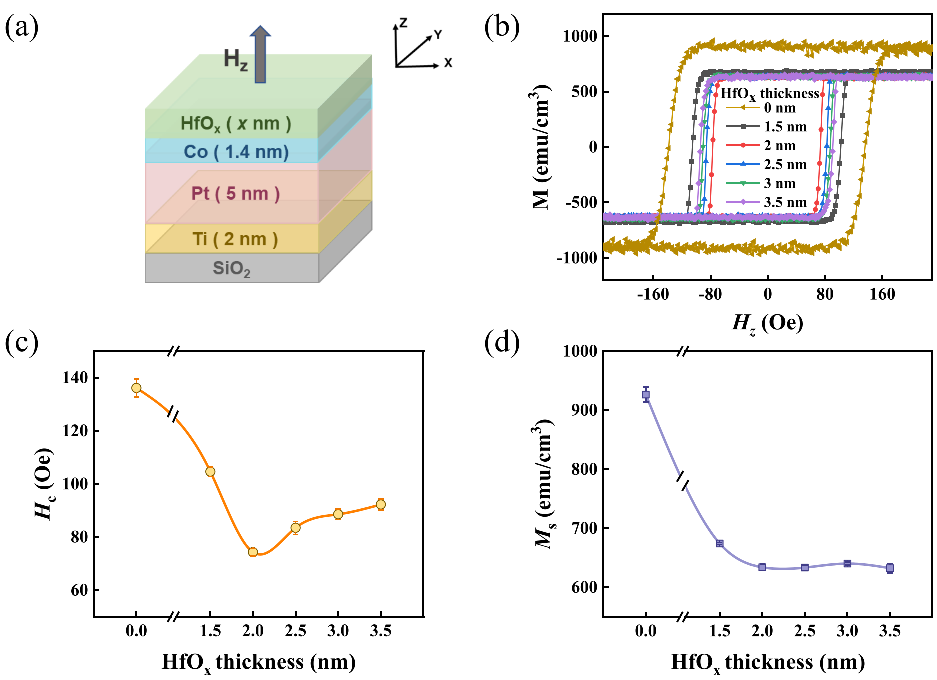

FIG. 1. (a) Schematic illustration of the Ti/Pt/Co/HfO_x multilayer. (b) Out-of-plane hysteresis loops of the Pt/Co/HfO_x stack with different HfO_x thicknesses. (c) The coercivity H_c and (d) the saturation magnetization M_s with different thicknesses of the HfO_x layer in the Pt/Co/HfO_x stack.

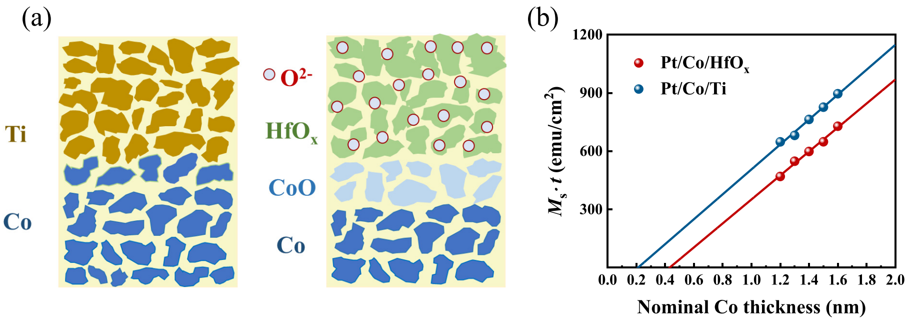

FIG. 2. (a) Schematic illustration of the process of oxygen migration to form CoO_x in the Co/HfO_x interface. (b) Magnetic dead layer obtained by varying the Co thickness with the HfO_x and Ti capping layers.

$$H_{DL} = -2\frac{H_L \pm 2\xi H_T}{1-4\xi^2}, \tag{1}$$

where H_L and H_T are defined as $H_{L,\pm} = (dV_{2\omega,x\pm}/dH_x)/(d^2V_{1\omega,x\pm}/dH_x^2)$ and $H_{T,\pm} = (dV_{2\omega,y\pm}/dH_y)/(d^2V_{1\omega,y\pm}/dH_y^2)$, respectively. ξ is the ratio of the planar Hall resistance and anomalous Hall resistance (R_{PHE}/R_{AHE}), determined to be 0.38 and 0.31 in the $Pt/Co/HfO_x$ and control samples, respectively. By fitting the experimental Hall voltage results under different current densities J_{ac} between 11×10^{10} and 15×10^{10} A/m^2, the corresponding damping-like field (H_{DL}) in Fig. 3(d) was obtained. The effective damping-like fields of both samples show good linearity with current density J_{ac}, where J_{ac} is the average current density. By fixing the intercept at zero and linearly fitting H_{DL} vs J_{ac}, the damping-like effective field efficiency was derived as $\chi_{DL} = H_{DL}/J_{ac}$. (The fitting details are shown in supplementary material Sec. S1.) For the $Pt/Co/HfO_x$ sample, the H_{DL} efficiency χ_{DL} is $(8.2 \pm 0.5) \times 10^{-10}$ Oe/(A/m^2), 60% higher than the control sample at $(5.1 \pm 0.9) \times 10^{-10}$ Oe/(A/m^2). The DL SOT efficiency is defined as follows:[16]

$$\xi_{DL}^{J_{ac}} = \frac{2e\mu_0 M_s t}{\hbar}\frac{H_{DL}}{J_{ac}}. \tag{2}$$

For the HfO_x sample, $\xi_{DL}^{J_{ac}}$ is 0.224 ± 0.014, 23% higher than the control sample at 0.181 ± 0.032. Subsequently, the effects of the enhanced SOT efficiency on the current-induced magnetization switching (CIMS) were investigated. The CIMS loops measured by using a series of DC pulses under an external in-plane magnetic field of ± 500 Oe are shown in Figs. 3(e) and 3(f). The pulse current was applied along the x-direction with a maximum magnitude of 25 mA and a duration

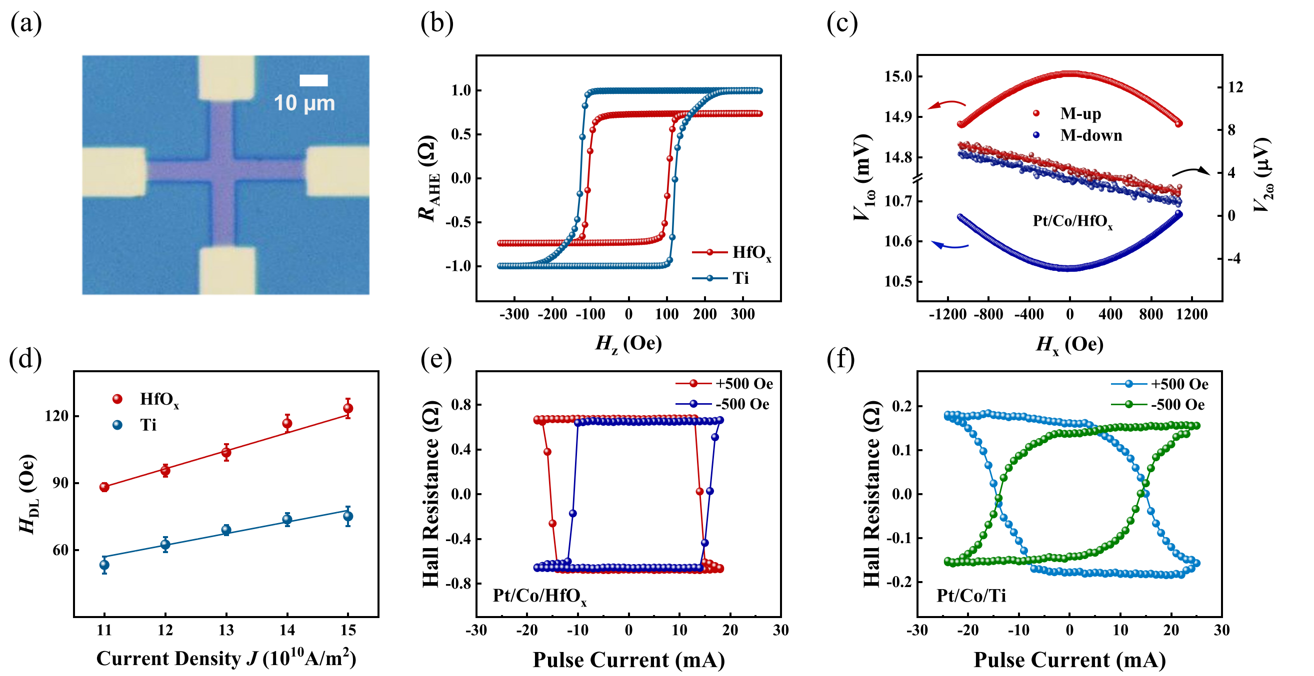

FIG. 3. (a) Optical micrograph of the patterned Hall bar device. (b) Anomalous Hall resistance loops measured on $Pt/Co/HfO_x$ and control devices under an out-of-plane field. (c) First and second harmonic Hall voltages as a function of an external in-plane magnetic field for the $Pt/Co/HfO_x$ device. M-up and M-down correspond to the sample magnetized initially along the $\pm z$ orientation. (d) Effective damping-like field as a function of the applied current density. Current-induced magnetization switching of (e) $Pt/Co/HfO_x$ and (f) control samples under the external in-plane magnetic field of ± 500 Oe.

of 5 ms. The average switching current for the Pt/Co/HfO_x sample was 14 mA, 14% lower than the control sample at 16 mA. The mechanism of CIMS involves the nucleation of the domain wall and the depinning of the domain wall. The switching current is not only related to the SOT efficiency but also the depinning field of the domain wall. In our experiments, we observed that the decrease in the switching current by 14% is not consistent with its coercivity change of 30%, which can be attributed to the natural defects and high pinning field of the Pt/Co/HfO_x sample.

To further understand how interfacial oxidation at the Co/HfO_x interface affects SOT efficiency, devices were fabricated for the voltage-gated measurement. This was achieved through the deposition of an additional HfO_x with a thickness of 50 nm on top of the Hall cross structure as the dielectric layer, followed by Ti (10 nm)/Cu (50 nm)/Ti (10 nm) deposited as a gate electrode. The schematic of the voltage-gated device and electrical measurement setup is shown in Fig. 4(a). The electric field between the top electrode and the Co layer is generated by applying gate voltages V_{gate} ranging between −4 and 4 V. Note that the negative gate voltages form an electric field that drives O^{2-} migration downwards from the HfO_x layer into the Co layer.[29] To estimate the electric field effect, the R_{AHE} was measured in the presence of various applied gate voltages, i.e., from 0 → −4 → 0 → 4 V with the step of 1 V. As shown in Fig. 4(b), the R_{AHE} loops under different gate voltages reveal that H_c decreases by 15%, from 135 to 117 Oe, when applying V_{gate} from 0 to −4 V. However, the R_{AHE} loop remains almost unchanged under the positive gate voltages. The gate voltage dependence of H_c is shown in Fig. 4(c). The change of the H_c is mainly attributed to the change of the *d* state electron density of Co.[21,35,36] Subsequently, the nonvolatility of the gate effect was checked by applying a gate voltage of −4 V for 10 min, then switching off the gate voltage. There was no change in the R_{AHE} vs H_z curves with $V_{gate} = -4$ V and $V_{gate} = 0$ V (−4 V → 0 V), which indicated that the gate effect is nonvolatile (as shown in supplementary material Sec. S3). Moreover, the anisotropy field H_k with gate voltages was investigated. The H_k was calculated from the parabolic fitting of R_{AHE} vs H_x curve. The normalized R_H can be written as

$$R_H^n = \frac{1}{2}\Delta R_H^n \cos(\theta), \quad (3)$$

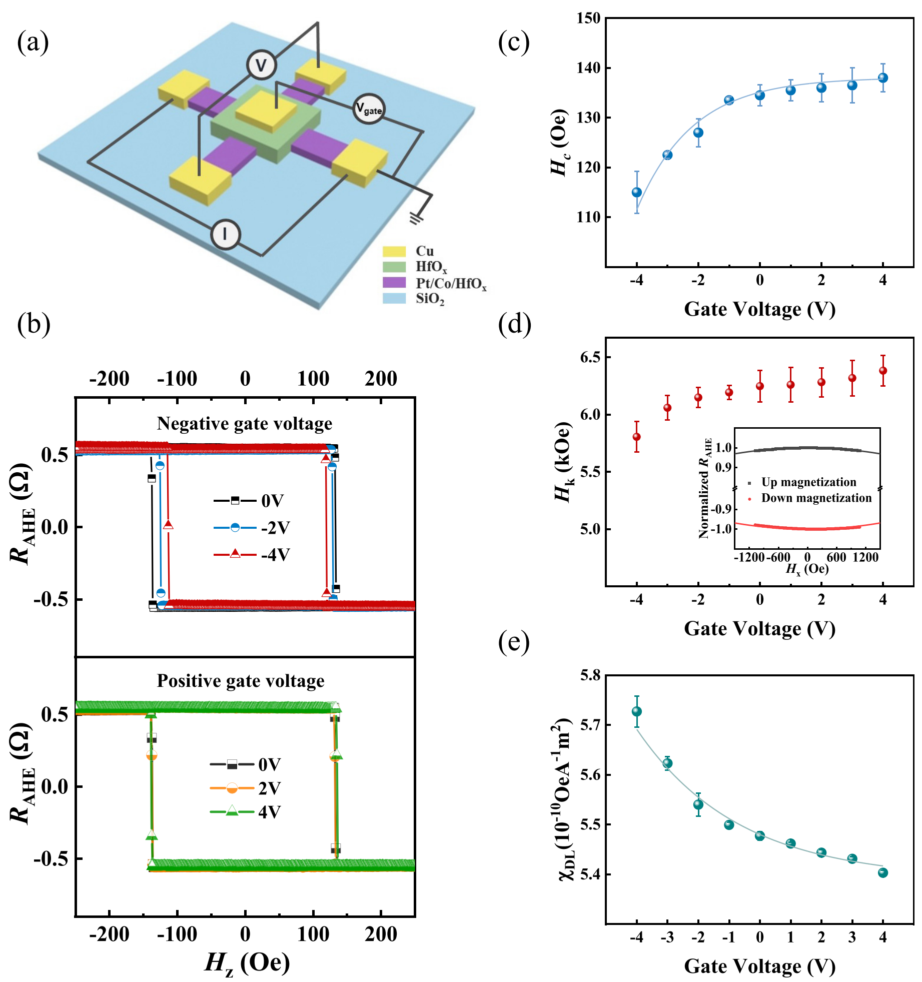

FIG. 4. (a) Schematic diagram of the voltage-controlled oxygen ion and electrical measurement setup. *I* is the applied current into the Hall cross. *V* is the measured Hall voltage in the crossbar. V_{gate} is the applied gate voltage. (b) Anomalous Hall resistance measured at $V_{gate} = -4$, −2, 0, 2, and 4 V with an out-of-plane magnetic field. (c) Coercivity H_c dependence on the gate voltage V_{gate}. (d) Magnetic anisotropy H_k dependence on the gate voltage V_{gate}, extracted from the normalized R_{AHE}. The inset shows the fitted R_{AHE} vs H_x. (e) The damping-like field SOT efficiency χ_{DL} at different gate voltages V_{gate}.

where R_H^n is the normalized Hall resistance and ΔR_H^n is the maximum resistance change between the up and down magnetization states. Hence, the value of $\Delta R_H^n = 2$. By utilizing the Maclaurin expansion and excluding high-order terms, Eq. (3) can be rewritten as

$$R_H^n = 1 - \frac{1}{2}\theta^2 = 1 - \frac{H_x^2}{2H_k^2}. \quad (4)$$

By fitting the parabolic curve of the first harmonic resistance with the H_x field, we obtained the H_k.[37] Across the gate voltage range of −4 to 4 V, H_k changes by about 10.1%, as shown in Fig. 4(d). The dependence of the SOT efficiency on the applied gate voltages is shown in Fig. 4(e). Similar to the R_{AHE} loop behavior, we observed the H_{DL} efficiency changing under negative V_{gate}, varying about 7%, but negligible changes under positive V_{gate}. Because the original Co layer has relatively low amount of oxygen atoms, there is negligible oxygen migration when the positive voltage is applied. Hence, the change in SOT efficiency is insignificant. Moreover, negligible changes were observed in the H_{FL} efficiency under V_{gate} (as shown in supplementary material Sec. S4). A larger electric field enables more oxygen migration to form CoO_x, which enhances the SOT efficiency. Interfacial orbital hybridization induced by interfacial oxygen migration results in SOT enhancement. This modification of SOT efficiency by gate voltages can also be understood from the enhancement of the spin transparency of CoO_x and the interfacial spin–orbit coupling strength.[23]

In conclusion, we have experimentally demonstrated the enhancement of damping-like effective fields and damping-like SOT efficiency by 60% and 23%, respectively, using the HfO_x capping layer in the Pt/Co system. The oxidization of the Co layer due to an oxide capping layer leads to an increase in SOT. Additionally, the use of gate voltages to tune the SOT efficiency by controlling interfacial oxygen ion migration has been demonstrated. SOT efficiency improves with increasingly negative gate voltages that drive oxygen ions into the Co layer but remains almost unchanged under positive gate voltages. This study unravels interfacial oxidation-based SOT enhancement by exploiting oxygen ion migration, which is useful in the development of highly energy-efficient spintronic devices.

See the supplementary material for the effective field-like field data, the nonvolatility of the gate effect, and anomalous Hall resistance measurements with different devices.

This work was supported by RIE2020 ASTAR AME IAF-ICP (Grant No. I1801E0030) and EDB-IPP (Grant No. RCA-2019-1376).

AUTHOR DECLARATIONS

Conflict of Interest

The authors have no conflicts to disclose.

Author Contributions

Shuo Wu: Conceptualization (equal); Data curation (equal); Formal analysis (equal); Investigation (equal); Methodology (equal); Writing – original draft (equal); Writing – review & editing (equal). **Tian Li Jin:** Conceptualization (equal); Formal analysis (equal); Investigation (equal); Writing – review & editing (equal). **Fu Nan Tan:** Formal analysis (equal); Software (equal). **Calvin Ching Ian Ang:** Writing – review & editing (equal). **Han Yin Poh:** Methodology (equal). **Gerard Joseph Lim:** Writing – review & editing (equal). **Wen Siang Lew:** Funding acquisition (lead); Supervision (lead); Writing – review & editing (equal).

DATA AVAILABILITY

The data that support the findings of this study are available from the corresponding author upon reasonable request.

REFERENCES

[1]S. A. Wolf, D. D. Awschalom, R. A. Buhrman, J. M. Daughton, S. von Molnár, M. L. Roukes, A. Y. Chtchelkanova, and D. M. Treger, Science **294**, 1488 (2001).
[2]M. Cubukcu, O. Boulle, N. Mikuszeit, C. Hamelin, T. Brächer, N. Lamard, M.-C. Cyrille, L. Buda-Prejbeanu, K. Garello, I. M. Miron, O. Klein, G. de Loubens, V. V. Naletov, J. Langer, B. Ocker, P. Gambardella, and G. Gaudin, IEEE Trans. Magn. **54**, 9300204 (2018).
[3]K. Garello, I. M. Miron, C. O. Avci, F. Freimuth, Y. Mokrousov, S. Blügel, S. Auffret, O. Boulle, G. Gaudin, and P. Gambardella, Nat. Nanotechnol. **8**, 587 (2013).
[4]L. Liu, C.-F. Pai, Y. Li, H. W. Tseng, D. C. Ralph, and R. A. Buhrman, Science **336**, 555 (2012).
[5]L. Liu, O. J. Lee, T. J. Gudmundsen, D. C. Ralph, and R. A. Buhrman, Phys. Rev. Lett. **109**, 096602 (2012).
[6]J. Cao, Y. Chen, T. Jin, W. Gan, Y. Wang, Y. Zheng, H. Lv, S. Cardoso, D. Wei, and W. S. Lew, Sci. Rep. **8**, 1355 (2018).
[7]V. M. Edelstein, Solid State Commun. **73**, 233 (1990).
[8]V. P. Amin, J. Zemen, and M. D. Stiles, Phys. Rev. Lett. **121**, 136805 (2018).
[9]C. Safranski, E. A. Montoya, and I. N. Krivorotov, Nat. Nanotechnol. **14**, 27 (2019).
[10]D. D. Awschalom and M. E. Flatté, Nat. Phys. **3**, 153 (2007).
[11]I. Mihai Miron, G. Gaudin, S. Auffret, B. Rodmacq, A. Schuhl, S. Pizzini, J. Vogel, and P. Gambardella, Nat. Mater. **9**, 230 (2010).
[12]T. Jin, W. C. Law, D. Kumar, F. Luo, Q. Y. Wong, G. J. Lim, X. Wang, W. S. Lew, and S. N. Piramanayagam, APL Mater. **8**, 111111 (2020).
[13]J. Kim, J. Sinha, M. Hayashi, M. Yamanouchi, S. Fukami, T. Suzuki, S. Mitani, and H. Ohno, Nat. Mater. **12**, 240 (2013).
[14]F. Freimuth, S. Blügel, and Y. Mokrousov, Phys. Rev. B **92**, 064415 (2015).
[15]C. O. Avci, K. Garello, C. Nistor, S. Godey, B. Ballesteros, A. Mugarza, A. Barla, M. Valvidares, E. Pellegrin, A. Ghosh, I. M. Miron, O. Boulle, S. Auffret, G. Gaudin, and P. Gambardella, Phys. Rev. B **89**, 214419 (2014).
[16]Y. Hibino, T. Hirai, K. Hasegawa, T. Koyama, and D. Chiba, Appl. Phys. Lett. **111**, 132404 (2017).
[17]C.-G. Duan, J. P. Velev, R. F. Sabirianov, Z. Zhu, J. Chu, S. S. Jaswal, and E. Y. Tsymbal, Phys. Rev. Lett. **101**, 137201 (2008).
[18]M. Oba, K. Nakamura, T. Akiyama, T. Ito, M. Weinert, and A. J. Freeman, Phys. Rev. Lett. **114**, 107202 (2015).
[19]T. Maruyama, Y. Shiota, T. Nozaki, K. Ohta, N. Toda, M. Mizuguchi, A. A. Tulapurkar, T. Shinjo, M. Shiraishi, S. Mizukami, Y. Ando, and Y. Suzuki, Nat. Nanotechnol. **4**, 158 (2009).
[20]K. Nakamura, T. Akiyama, T. Ito, M. Weinert, and A. J. Freeman, Phys. Rev. B **81**, 220409 (2010).
[21]F. Bonell, Y. T. Takahashi, D. D. Lam, S. Yoshida, Y. Shiota, S. Miwa, T. Nakamura, and Y. Suzuki, Appl. Phys. Lett. **102**, 152401 (2013).
[22]I. M. Miron, K. Garello, G. Gaudin, P.-J. Zermatten, M. V. Costache, S. Auffret, S. Bandiera, B. Rodmacq, A. Schuhl, and P. Gambardella, Nature **476**, 189 (2011).
[23]X. Qiu, K. Narayanapillai, Y. Wu, P. Deorani, D.-H. Yang, W.-S. Noh, J.-H. Park, K.-J. Lee, H.-W. Lee, and H. Yang, Nat. Nanotechnol. **10**, 333 (2015).
[24]K.-U. Demasius, T. Phung, W. Zhang, B. P. Hughes, S.-H. Yang, A. Kellock, W. Han, A. Pushp, and S. S. P. Parkin, Nat. Commun. **7**, 10644 (2016).
[25]S. Emori, U. Bauer, S. Woo, and G. S. D. Beach, Appl. Phys. Lett. **105**, 222401 (2014).
[26]L. Yang, Y. Fei, K. Zhou, L. Chen, Q. Fu, L. Li, C. Yan, H. Li, Y. Du, and R. Liu, Appl. Phys. Lett. **118**, 032405 (2021).

[27]J. Xu and C. L. Chien, Appl. Phys. Lett. **118**, 052409 (2021).
[28]C. Song, B. Cui, F. Li, X. Zhou, and F. Pan, Prog. Mater. Sci. **87**, 33 (2017).
[29]T. Hirai, Y. Hibino, K. Hasegawa, M. Kohda, T. Koyama, and D. Chiba, Appl. Phys. Express **13**, 123005 (2020).
[30]T. Hirai, T. Koyama, A. Obinata, Y. Hibino, K. Miwa, S. Ono, M. Kohda, and D. Chiba, Appl. Phys. Express **9**, 063007 (2016).
[31]M. Hayashi, J. Kim, M. Yamanouchi, and H. Ohno, Phys. Rev. B **89**, 144425 (2014).
[32]W. Lv, H. Xue, J. Cai, Q. Chen, B. Zhang, Z. Zhang, and Z. Zeng, Appl. Phys. Lett. **118**, 052406 (2021).
[33]K. Hasegawa, Y. Hibino, M. Suzuki, T. Koyama, and D. Chiba, Phys. Rev. B **98**, 020405 (2018).
[34]H. Y. Poh, C. C. I. Ang, W. L. Gan, G. J. Lim, and W. S. Lew, Phys. Rev. B **104**, 224416 (2021).
[35]J. Suwardy, K. Nawaoka, J. Cho, M. Goto, Y. Suzuki, and S. Miwa, Phys. Rev. B **98**, 144432 (2018).
[36]M. Endo, S. Kanai, S. Ikeda, F. Matsukura, and H. Ohno, Appl. Phys. Lett. **96**, 212503 (2010).
[37]F. N. Tan, Q. Y. Wong, W. L. Gan, S. H. Li, H. X. Liu, F. Poh, and W. S. Lew, J. Magn. Magn. Mater. **485**, 174 (2019).